DOI: 10.21062/mft.2024.015 http://www.journalmt.com

Analysis of the Basic Characteristics of the Working Accuracy of the Atomic Diffusion Additive Manufacturing ADAM Process by Comparison with the Selective Laser Melting SLM Process

Andrej Czan (0000-0002-8826-1832)[1], Tatiana Czanova (0000-0002-6943-6393)[1], Jozef Holubjak (0000-0003-3226-9445)[1], Martin Novak (0000-0002-2010-4398)[2], Natalia Czanova (0009-0005-3047-130X)[1], Andrej Czan (0009-0003-9588-4530)[1], Dominik Krisak (0009-0005-3742-272X)
[1]Department of Machining and Production Engineering, Faculty of Mechanical Engineering - University of Žilina, Univerzitna8215/1, 010 26, Žilina, SLOVAKIA. E-mail: andrej.czanstroj.uniza.sk
[2]Faculty of Mechanical Engineering, Jan Evangelista Purkyne University in Usti nad Labem, Pasteurova 3334/7, 400 01 Usti nad Labem. Czech Republic.

Atomic Diffusion Additive Manufacturing (ADAM) is a progressive layering process based on metallic materials with a plastic binder designed to extrude the material. The ADAM process can be classified as an indirect additive manufacturing process in which a solid fiber of metal powder enclosed in a plastic binder is applied. After creating a 3D object by the ADAM process, the excess plastic binder is removed in the cleaning chamber and vacuum sintering of the 3D object is performed. This work aims to provide a preliminary characterization of the ADAM process and compare the achieved results with the application most recently implemented in additive manufacturing for metal 3D objects using Selective Laser Melting SLM. In particular, the density and microstructure of the applied process and material 17-4PH are studied, while optimal or recommended technological parameters of production facilities are applied. Furthermore, the dimensional accuracy of the ADAM process is observed, which is evaluated using IT accuracy levels according to the ISO reference artifact. Due to the applied AM process, the final character of a 3D object depends on technological parameters. The weight of a 3D object is low compared to the material processed by additive manufacturing processes in a powder bed. The dimensional accuracy and roughness of the surface depend on the geometry, orientation, and position of the individual shape specifications of the 3D object. Additive technologies generally achieve a degree of accuracy of approximately IT12 to IT13, which is comparable to traditional semi-finished metal manufacturing processes.

Keywords: Additive Manufacturing, Metal 3D Objects, Dimensional Accuracy, Shape Accuracy, Surface Roughness

1 Introduction

Additive manufacturing (AM) processes are causing a revolution in the way engineers and designers can conceive and produce products, thanks to greater design freedom. Since the inception of rapid prototyping (RP) systems at the end of the last century, additive manufacturing machines have been rapidly improving and evolving towards efficient systems for mass-producing customized products [1]. The absence of the need for specific tools or molds reduces the economic cost per unit. Especially in the case of metallic components, interest in the industry is growing exponentially because additive manufacturing enables the production of parts with nearly full density and complex structures made from excellent materials [2,3]. The main advantage of additive manufacturing over conventional subtractive or formative methods is the demonstrated higher product functionality that can be achieved by utilizing design freedom effectively[4].

Additive manufacturing processes developed for metallic components are primarily based on powder bed technology, wherein energy is used to melt the material selectively [1]. Due to the inefficiency and low power output of energy sources, the earliest metallic additive machines were only indirect production systems, as additional post-processing was required to achieve a part with relatively good mechanical performance. In these initial processes, metallic powder was mixed with a polymer binder[5].

The source of energy from a laser beam was utilized to melt the binder, which served as an aggregator for metallic particles. The compressed portion, consisting of both the binder and metallic materials, was referred to as the "green part." The binder had to be removed through additional heat treatment. Residual porosity, sometimes as high as 40%, was addressed by infiltrating with copper or bronze [6,7]. Examples of such indirect additive

manufacturing processes include 3D printing or selective laser sintering (SLS). Later, EOS developed a direct metal laser sintering (DMLS) system, eliminating the need for polymer binders as the implemented laser power was sufficient to directly sinter low-melting alloys. In this case, the residual porosity, which required filling by infiltrating with another material, was lower at around 20% [6]. Recent advancements in higher-power energy sources have allowed engineers to overcome these initial limitations and unleash the technological potential. Currently, a broader range of metals can be processed directly through additive manufacturing to obtain dense metallic parts without any additional post-processing. Laser or electron beam sources fully melt the metal powder [8], resulting in a fully dense (over 99.9%) part. In some cases, the mechanical properties of additively manufactured parts are even superior to their corresponding cast material. Furthermore, due to controlled build chambers, materials with high melting points and/or oxygen affinity, such as titanium alloys, can be more easily processed by additive manufacturing than conventional methods [8]. However, powder-based additive processes present certain design constraints related to the feasibility of enclosed cavities. In fact, after construction, unprocessed powder around the part needs to be removed through mechanical or manual operations. Enclosed cavities inaccessible from the outside are, therefore, not allowed. This limitation restricts the design of lightweight parts that might include enclosed lattice structures to provide stiffness without increasing weight under load. The use of powders also poses challenges for applying powder bed processes in extreme manufacturing scenarios, such as zero-gravity environments [9], where powder management is impractical. To overcome these limitations, additive manufacturing processes based on extrusion have recently been developed and introduced to the market. They draw inspiration from wire welding processes and fused deposition modeling (FDM) techniques, extensively used in the layer-by-layer production of polymer and composite parts. Compared to other additive manufacturing processes, extrusion-based processes are more user-friendly, and their equipment is more cost-effective. Moreover, these systems are suitable for multi-material deposition. Electron Beam Additive Manufacturing (EBAM) is a direct additive manufacturing process for large-scale metallic components, where a metallic wire is extruded while being melted by an electron beam [8]. Its primary applications range from rapid prototyping to production parts and component repairs. American companies Desktop Metal Inc. and Markforged Inc. [10,11] have recently introduced two new machines based on a combination of fused deposition modeling (FDM) for polymers and metal injection molding (MIM) for metals [12], a traditional process for obtaining near-net-shape metallic parts with high complexity [13]. Desktop Metal's patented process is called Bound Metal DepositionTM (BMD), while Markforged Inc. named their process Atomic Diffusion Additive Manufacturing (ADAM). Both processes use a filament made of metallic powders encapsulated in a thermoplastic polymer that acts as a binder for the metal particles [14]. The mixture (metal powder particles and polymer) is stored in a cartridge on top of the machine and is introduced into the unit during the process, where the thermoplastic is softened for easy extrusion. BMD employs an ultrasonic vibrator to provide the necessary energy to bond the extruded material with the previously deposited material [14], while Markforged Inc. utilizes a simple heated extruder [11]. The softened material accumulates and is then pushed through a nozzle or extruder by a piston, layer by layer onto the build platform [14]. Similar to the MIM process, the as-built part, also called the "green part," is washed to remove the binder (debinding or leaching operation) and then sintered in a furnace to achieve material densification (sintering). Figure 1 illustrates the schematic workflow of the process. The binder used in Markforged Inc.'s system is thermally debound in a washing system before the sintering phase [15]. In Desktop Metal's system, the binder is first debound using a solvent and then thermally treated [15]. Due to the presence of the binder and the sintering phase, the part must be oversized and dimensionally adjusted to account for shrinkage during subsequent processing.

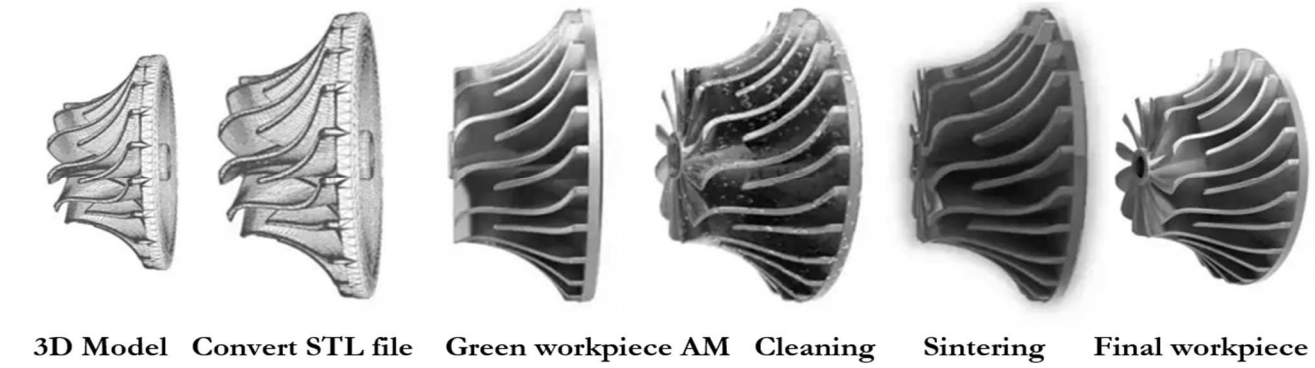

Fig. 1 *Atomic Diffusion Additive Manufacturing (ADAM) workflow*

The aim of this work is to provide basic characteristics of the working precision of the ADAM process using technological equipment Markforged Metal X, which is unique in complex model design up to the final product. In the analysis of working accuracy, the available material of 17-4 PH, which is a debugging material by Markforged for industrial application, was considered. The working accuracy is examined on the final samples, which have different object topologies. Dimensional and shape accuracy, and surface roughness, which are measured on different sample areas, are monitored. The working accuracy of the ADAM process is evaluated and defined by IT ISO grades using a reference artifact from the literature.

2 Materials and methods

2.1 Material and equipment for the process ADAM

In 2017, Markforged Inc. launched the Metal X technological equipment, its heat device (own) for additive manufacturing of metal components (AM). The nominal composition of Markforged 17-4 PH is shown in Table 1 [16]. The 17-4PH material offers high strength and hardness along with excellent corrosion resistance. It is used in a variety of applications including oil field valve parts, chemical process equipment, aircraft structural parts, fasteners, pump shafts, nuclear reactor components, gears, paper mill equipment, rocket equipment jet engine parts, etc. The 17-4 PH material itself is a registered trademark of AK Steel.

The construction space of the technological equipment is 300 × 220 × 180 mm, which represents a volume of 11880 cm3, but the maximum size of the part that can be built is 250 × 183 × 150 mm. At the beginning of each work, a vacuum-sealed sheet is placed on top of the construction platform, which facilitates the adhesion of the part during construction and its separation at the end of the process. The base plate and leveling system are designed to support a maximum load of up to 10 kg. The interior space of the device and the baseplate are heated to specified temperatures during the process. The cleaning process is carried out in a washing system with a volume of 18356 cm3 in a whirlpool bath with washing liquid Opteon Zion. The sintering process itself is carried out in a Sinter-2 vacuum furnace with a volume of 18356 cm3. In the furnace, we can reach a temperature of up to 1300oC and can work in an inert atmosphere using argon and nitrogen. The chamber has a cylindrical volume with a diameter of 248 mm and a length of 406 mm.

The size of the part and the entire parameters of the ADAM process, including the supporting structure, are designed automatically by proprietary software called Eiger. Eiger is a CAM software that controls the entire process from design to the sintering stage. The software is closed to the user. Therefore, the process parameters are unknown and cannot be changed by the user, except for the layer thickness, which represents the resolution of the machine. The layer thickness can be adjusted from 0.085 mm to 0.175 mm. The set layer height for experimental samples was 0.100 mm. After adjusting the layer thickness, Eiger software calculates the volume increase to account for part shrinkage during post-print operations. It then provides the final geometry and shape to be printed, as well as the time required to infuse the polymer (cleaning time). Eiger software also defines heat treatment for the next sintering step [17,19,20].

Tab. 1 *Chemical composition in wt% of material 17-4 PH*

Cr	Ni	Cu	Si	Mn	Nb	C	P	S	Fe
16.23	4.2	3.8	0.94	0.87	0.38	0.032	0.026	0.015	Bal

2.2 Material and equipment for the SLM process

SLM (Selective Laser Melting) technology uses a powerful energy laser beam to produce parts, which melts the material in powder form layer by layer until the desired shape is achieved. The technology uses a metallic material in the form of powder, which is evenly applied to the platform, where it is subsequently fused with a powerful laser on the desired area. Using a short pulse, the laser fuses a thin layer of material so that the individual parts connect tightly enough, creating the first layer of a 3D object. When the process is complete, it is necessary to clean the formed solidified part from the remnants of non-stick powder particles of the material.

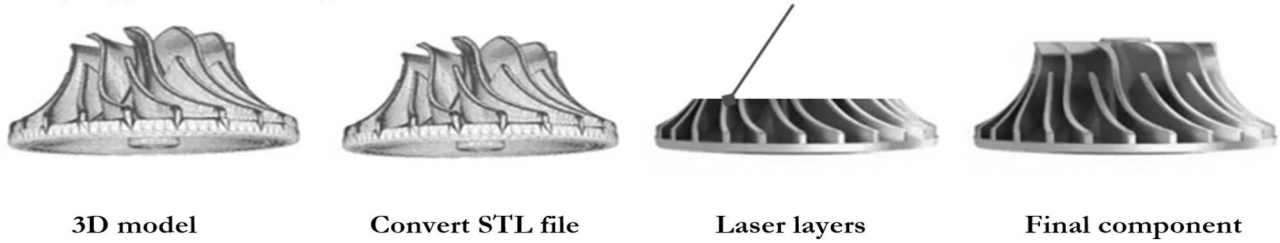

Fig. 2 *Selective Laser Melting (SLM) workflow*

The material applied in the production of experimental samples was the same as in the ADAM 17-4PH process. The chemical composition of the material was the same mass fraction according to the standard. Samples after the layering process were sandblasted to remove excess metal powder.

2.3 Design of experimental samples

The basis for the design of the experimental sample is based on the generation of reference areas in the orientation of the coordinate systems X, Y, and Z. Due to the applied AM technologies, we know that the formation of layers and their properties after curing show diversity. This diversity is influenced by the orientation of the sample location in the space of the building chambers X, Y, and Z and the orientation of the technological application of layers. In previous knowledge and experience, there are a large number of reference samples for contrast monitoring and creating detailed objects in AM technologies. However, these samples cannot account for the influence of individual orientations as well as layering directions of 3D models.

For overall volume or spatial analysis in three-dimensional orientation, it is advisable to design the sample so that it takes into account all orientations, but also areas that are in both positive and negative angles in Z orientation. Therefore, the sample was designed in a three-dimensional orientation, where areas in an octagonal shape are created, where all faces of a given model are at the same distance and are parallel to each other in Figure 3. All parallel faces have a distance of 30mm, hole samples have a hole diameter of 5mm, and threaded samples have an M6 thread.

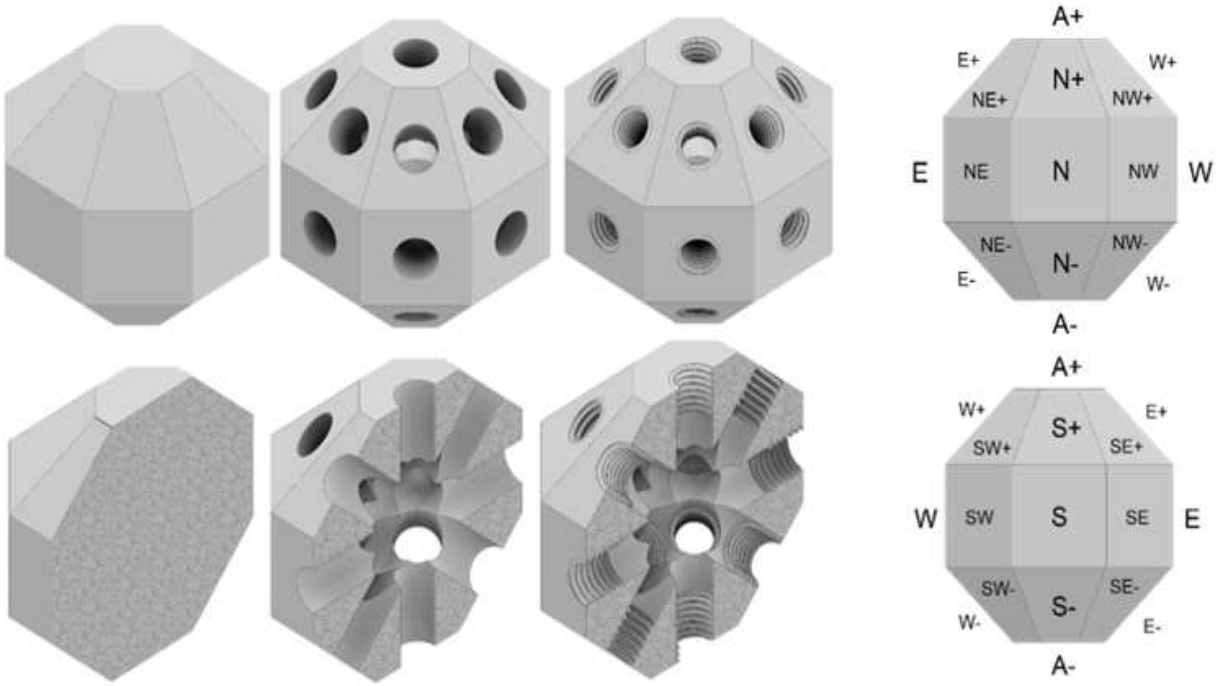

Fig. 3 *View 3D models of samples in full shape (P) with holes (D) and threads (Z) and view of the detail of the samples in the section, where the NSEW+/-A system of marking the monitored areas is shown on the right*

The design of the sample has eight square areas in plane XY. In the Z orientation, there are two parallel octagonal faces marked as areas in positive and negative inclination. Due to the formation of surfaces connecting square and octagonal surfaces, trapezoidal surfaces are formed, the slope of which is either in positive or negative orientation. In total, the proposed sample has 26 surfaces that are parallel to each other, thus creating a 26-sided spherical object of the Revolved Sphere type. The proposed samples ensured the identification of working accuracy when creating samples in which dimensional and shape specifications and surface roughness could be analyzed.

3 Evaluation of experimental trials

3.1 Evaluation of real samples and surface texture

According to the design, real samples were produced, which were in full shape with holes made and threads made directly during layering. The samples were oriented according to the Cartesian coordinate system of Figure 3. The designation according to individual quadrants in space is rather opaque and therefore the orientation was on the simplified designation of the coordinate system, namely the X axis as the E-W axis, the Y axis as the N-S axis, and the Z axis as A+ and A-. The samples

have eight square faces in XY orientation marked according to directions NSEW+/-A and their combinations of 45° as NE, NW, SE, and SW. In the Z orientation, there are two parallel octagonal faces designated as faces A in positive (+) and negative (-) inclinations. The system was implemented to subsequently identify the individual created areas of a spherical object, where, based on applied marking, samples were produced at individual bases of technological equipment. Figure 4 shows the samples produced using SLM technology. The next figure 5 identifies objects from ADAM technology.

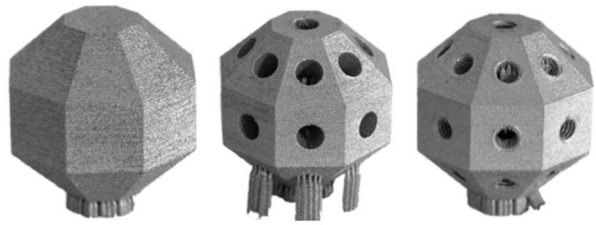

Fig. 4 *Realistically created identification experimental samples and their three variants plan P, with holes D and threads Z produced by SLM technology*

Fig. 5 *Realistically created identification experimental samples and their three variants plan P, with holes D and Z threads produced by ADAM technology*

To identify the created surfaces and their basic parameters of directness P, roughness R, and corrugation W, the Infinite Focus G5 device was applied. The Infinite Focus G5 is an optical measurement of microcoordinates and surface treatment measurement in one system. Infinite Focus is a highly accurate, fast, and flexible optical 3D measurement system. By applying the G5 system, we obtain a combined two-in-one system based on the integration of a 3D microcoordinate measuring machine and a device for measuring surface roughness. The range of measurable surfaces is almost unlimited. For microprecision components, all their relative surface properties are measured using one multifunctional measurement sensor. It allows you to achieve highly accurate and repeatable measurements with vertical resolution up to 10nm [17,19,22]. Using hardware-assisted vibration damping and focusing variation, this measurement principle can analyze the shape and surface roughness of large and heavy objects [20]. The axes on the Infinite Focus have built-in high-precision positioning devices that ensure precise movement of the ports in the X and Y planes [18,21,23]. Thanks to its automated interface, the Infinite Focus is also used for fully automatic measurements in production. The analyzed scanned areas in position 'S' are shown in Figure 6.

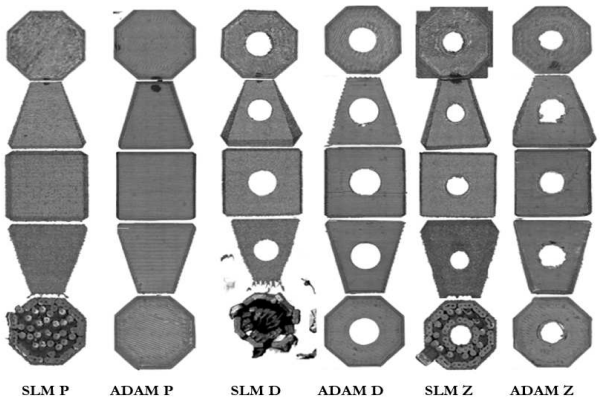

Fig. 6 *Images of scanning surfaces in the "S" position for experimental samples solid P, with holes D and with Z threads*

3.2 Evaluation of surface parameters P, R, and W

The primary mean arithmetic deviation of the profile was observed, which is considered, in our case Pa, Ra, Wa is determined as the mean arithmetic value of the absolute deviations of the profile Z(x) in the range of their basic length [22,24,29].

$$Pa, Ra, Wa = \frac{1}{l}\int_0^l /Z(x)/dx \ , \ for \ \mathrm{l} = \mathrm{lp, lr \ or \ lw} \quad [\mathrm{mm}] \tag{1}$$

The mean quadratic deviation of the considered profiles in our case profiles Pq, Rq, and Wq is determined as the mean quadratic value of the absolute deviations of the profile Z(x) in the range of their base length. [22,24,29]

$$the \ Pq, Rq, Wq = \sqrt{\frac{1}{l}\int_0^l Z(x)^2 \, dx} \ , \ \ \mathrm{for \ l = lp, lr \ or \ lw} \quad [\mathrm{mm}] \tag{2}$$

The total height Pz, Rz, Wz, is the sum of the maximum height of peak Zp and maximum depression Zv of the profile within the assessment length, not the sampling length. The Rt≧Rz relationship applies to all profiles. Pt Maximum total section height and Wt Maximum total corrugation height [22,24,29].

$$Pz, Rz, Wz = maxZp + maxZv \ , \ \ \mathrm{for \ l = lp, lr \ or \ lw} \quad [\mathrm{mm}] \tag{3}$$

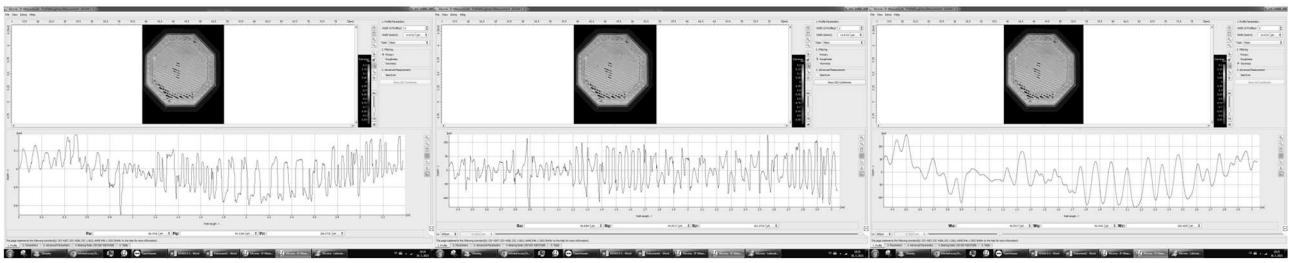

Fig. 7 *Model of evaluated surfaces for full sample and area A+, parameters Ra, Rq, and Rz identified*

The device was set up to identify samples, where the surface of samples produced by SLM and ADAM technologies was scanned in the form of a sample full (P), a hole model (D), and a threaded model (Z). On each of the samples, the areas A+, S+, S, S-, and A- were scanned to identify the surface in individual orientations. A sample of the scanning outputs is shown in Fig. 7. The parameters Pa, Ra, Wa, Pq, Rq, Wq, Pz, Rz, and Wz are evaluated. Comparison of scanned surfaces for all three kinds of experimental samples with surface analysis of the color map Fig. 8.

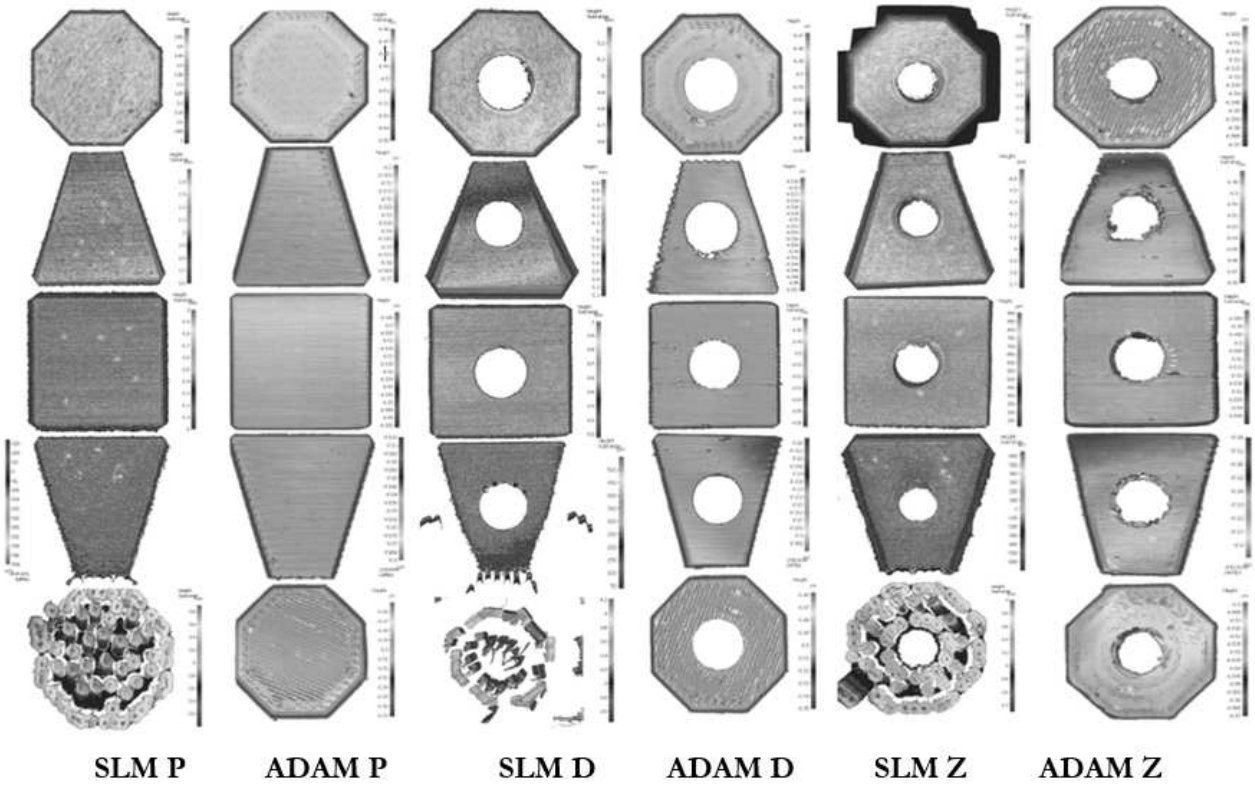

Fig. 8 *Images of scanning surfaces in the "S" position with texture identification via color map for experimental samples solid P, with holes D and with Z threads*

3.3 Methodology for evaluating working accuracy

The aim of the working accuracy analysis is to evaluate the dimensional and shape accuracy that can be obtained by the ADAM process. The analysis was performed using reference samples designed to identify the basic precision characteristics of AM processes(25). The reference part consists of the same simple geometries of different dimensions that characterize the accuracy of the first eight ranges of basic size and parallelism of each other's faces Fig. 3. Dimensional and geometric tolerances, including shape defects, are evaluated for the convex and concave properties of the artifact according to the system

The evaluation of the dimensional accuracy of the replica was carried out in accordance with Directive ISO 286-1:1988(26). For each ISO base size range, the dimensional accuracy of the ADAM process was evaluated concerning the achieved IT level of the replica artifact. In particular, the IT precision level has been defined assuming that the maximum dimensional error is the number of unit tolerances n corresponding to the 95th percentile of the

distribution of the number of unit tolerances nj for the general jth dimension, where nj is calculated as follows:

$$n_j = \frac{1000|D_{jn} - D_{jm}|}{i} \quad (4)$$

Where:

Djn…The nominal dimension,

Djm…The actual dimension of the character,

i…Tolerance factor that varies between different ranges of the basic ISO size (Table 2). The actual dimension is considered to be the average of three replications of the measurement of one geometric sign of the replica.

The measurements were made using the CMM Zeiss Eclipse coordinate measuring machine. The CMM model is GLOBAL Image 07.07.07, which has a declared maximum permissible error (MPEE) of 2.2 μm + L/1000 according to ISO-10360/2 [27], where L is the measured length. Table 3 shows the dimensional quality classification because ISO IT grades depend on n [28,29].

Tab. 2 *International Organisation for Standardisation (ISO) basic size ranges and corresponding tolerance factor i*

Range	Basic Size							
Above D_1 (mm)	1	3	6	10	18	30	50	80
Up to including D_2 (mm)	3	6	10	18	30	50	80	120
Standard tolerance factor *i* (μm)	0.542	0.733	0.898	1.083	1.307	1.561	1.856	2.173

Tab. 3 *Classification of IT levels according to ISO 286-1:1988*

Range		IT 10	IT 11	IT 12	IT 13	IT 14	IT 15	IT 16
Above 1 mm	Up to 500 mm	64i	100i	160i	250i	400i	640i	1000i

4 Results and discussion

After scanning individual surfaces using the InfiniteFocus G5 optical measuring device, summary comparisons of the achieved surface parameters were performed. Based on the results obtained, the effects of the solid P model with holes D and with threads Z for one technology were compared so that it was possible to monitor the influence of technology and shape of surfaces of models P, D, and Z on the resulting areas in individual orientations A+, S+, S, S-, A-. Subsequently, the results were compared between different technologies on surface properties. Figs. 7.6 to 7.11 summarize the measured deviations, their average values, as well as the standard deviation with the graphical polar display.

Based on the graphs, I can determine that the sample produced by Binder Jetting technology showed the best values from the samples examined. The sample produced by ADAM technology showed the best-achieved values at the Full Sample. SLM technology has achieved the least satisfactory values due to the added supports, the removal of which requires a further technological operation.

Pa (μm)	SLM	ADAM
A+	17.59	14.82
S+	97.47	36.576
S	22.90	42.72
S-	50.75	25.41
A-	79.48	93.96
Average	53.63	42.70
St. deviat.	34.79	30.58

Ra (μm)	SLM	ADAM
A+	7.17	4.59
S+	13.55	15.45
S	17.01	6.62
S-	25.19	11.95
A-	35.05	14.31
Average	19.60	10.64
St. deviat.	10.80	4.68

Wa (μm)	SLM	ADAM
A+	13.56	13.62
S+	86.37	31.40
S	12.42	17.51
S-	41.94	19.43
A-	69.15	83.08
Average	44.75	33.01
St. deviat.	32.90	28.76

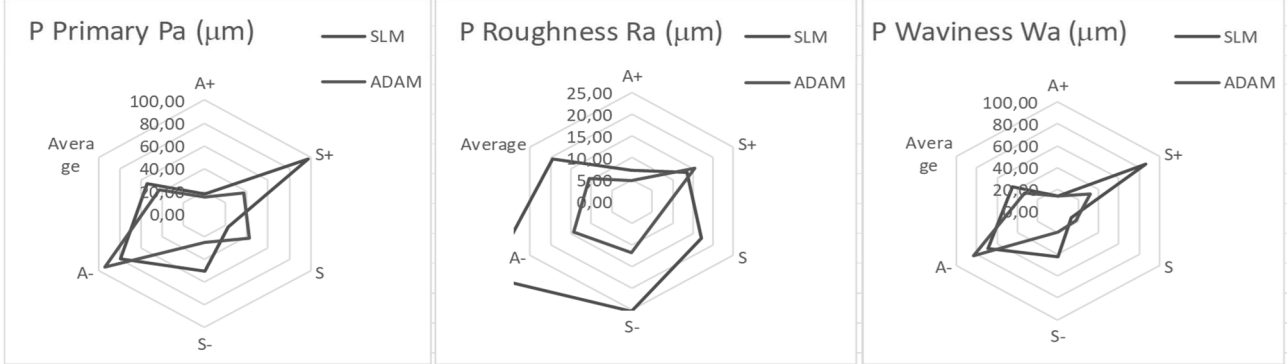

Fig. 9 *Evaluation of measured values of directness, roughness, and corrugation of profile Pa, Ra, Wa and their comparison in polar graphical representation for SLM and ADAM technologies of sample P*

Pa (μm)	SLM	ADAM
A+	60.00	74.34
S+	284.41	27.46
S	32.62	15.81
S-	68.99	89.77
A-	17.60	25.06
Average	92.72	46.49
St. deviat.	109.12	33.20

Ra (μm)	SLM	ADAM
A+	4.71	40.62
S+	8.47	9.73
S	7.78	5.87
S-	22.32	12.06
A-	27.71	5.16
Average	14.04	14.61
St. deviat.	10.31	14.80

Wa (μm)	SLM	ADAM
A+	51.50	43.39
S+	254.39	24.68
S	28.26	13.32
S-	53.29	74.99
A-	171.99	19.39
Average	111.89	35.15
St. deviat.	97.45	24.95

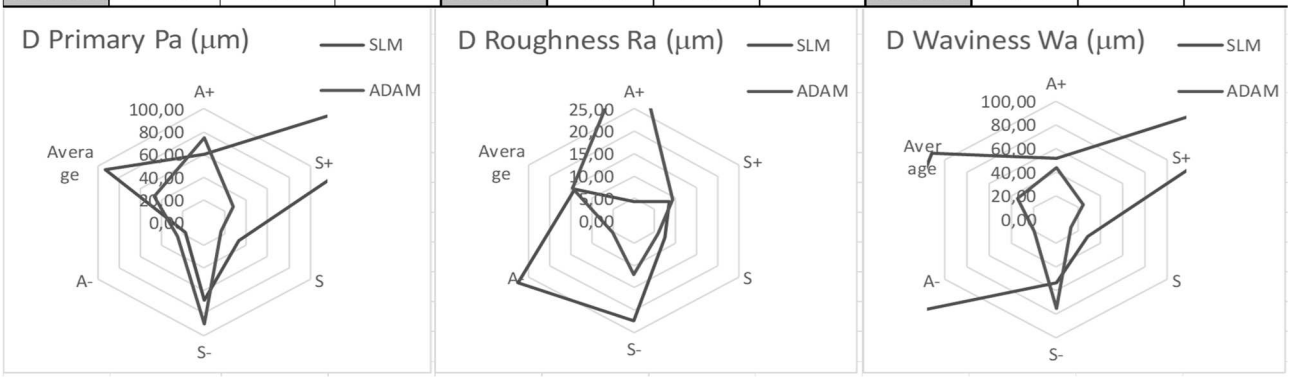

Fig. 10 *Evaluation of measured values of directness, roughness, and corrugation of profile Pa, Ra, Wa and their comparison in polar graphical display for SLM and ADAM technologies of sample D*

Pa (μm)	SLM	ADAM
A+	87.87	53.22
S+	50.82	125.89
S	44.10	13.65
S-	42.78	122.43
A-	412.01	49.69
Average	127.53	72.89
St. deviat.	160.09	49.24

Ra (μm)	SLM	ADAM
A+	5.32	4.94
S+	7.31	11.01
S	5.80	6.49
S-	23.79	9.87
A-	46.59	25.39
Average	17.76	11.54
St. deviat.	17.85	8.12

Wa (μm)	SLM	ADAM
A+	79.52	52.06
S+	45.10	120.37
S	39.61	10.14
S-	30.85	116.18
A-	420.87	36.21
Average	123.20	67.06
St. deviat.	167.43	49.07

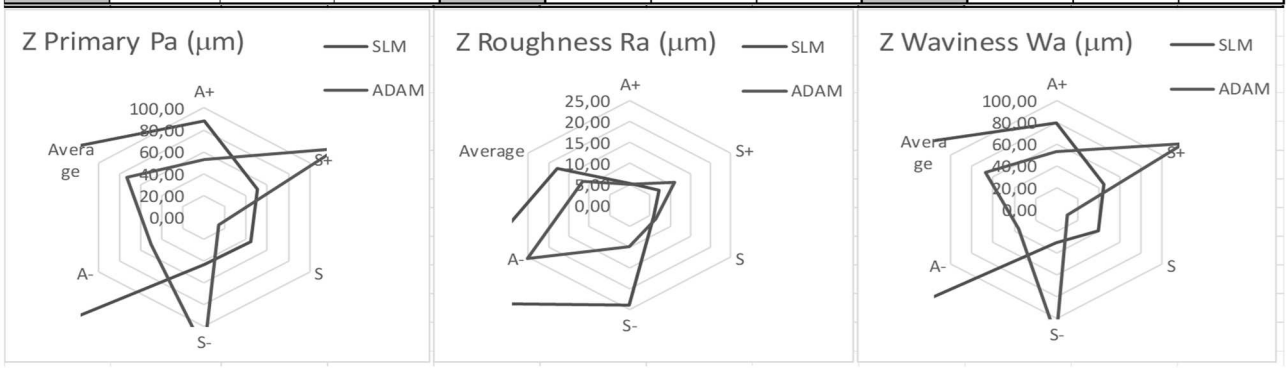

Fig. 11 *Evaluation of measured values of directness, roughness, and corrugation of the profile Pa, Ra, Wa and their comparison in polar graphical display for SLM and ADAM technologies of the Z sample*

The samples were analyzed using the Alicona InfinteFocus G5 confocal microscope measuring device, where a lens with a 5x magnification was applied. The graphs in Figures 9 to 11 show the individual samples examined produced by different AM technologies and compare their primary surface profile Pa, surface profile roughness Ra, and corrugation of surface profile Wa. Full samples performed better, the best of which was ADAM technology. Also, for samples with holes, ADAM obtained results were better. SLM technology achieved worse results due to the supports that were applied in the production of experimental samples. For the experimental threaded sample, ADAM technology showed measurement results similar to previous measurements for a full sample P and a sample with holes D. The best roughness values were achieved in the ADAM process.

The measured data were processed to determine the accuracy of applied AM technologies, namely SLM and ADAM. The upper and lower dimension limits with a set tolerance of ±0.2 mm were monitored, where the difference from tolerance was analyzed. Subsequently, the accuracy of the technology was monitored, such as the determination of the standard tolerance factor "i", average measured values, and determination of a deviation from the nominal size, where the tolerance range was subsequently

determined and subsequently the IT degree of accuracy was determined. The IT degree of accuracy was analysed for all measured values of individual surfaces, where minimum, average, and maximum tolerance ranges were compared. The results were compared in graphical representation on polar graphs for both applied AM technologies and their 3D models of various shapes P, D, and Z, Figs. 12 to 17.

AREA	IT range min. [mm]	IT range avg. [mm]	IT range max. [mm]	ITx min	ITx average	ITx max
A1/A2	40	71	165	IT9	IT10	IT12
N/S	71	90	120	IT10	IT11	IT11
NW/SE	119	137	154	IT11	IT12	IT12
W/E	155	188	207	IT12	IT12	IT13
SW/NE	116	169	221	IT11	IT12	IT13
N+/S-	144	101	64	IT12	IT11	IT10
N-/S+	85	60	36	IT11	IT10	IT9
NW+/SE-	96	48	11	IT11	IT9	IT6
NW-/SE+	100	56	31	IT11	IT10	IT8
W+/E-	46	6	35	IT9	IT5	IT9
W-/E+	48	41	35	IT9	IT9	IT9
SW+/NE-	83	37	18	IT11	IT9	IT7
SW-/NE+	139	87	50	IT12	IT11	IT9
Average	95	84	88	IT11	IT11	IT11
min	40	6	11	IT9	IT5	IT6
max	155	188	221	IT12	IT12	IT13

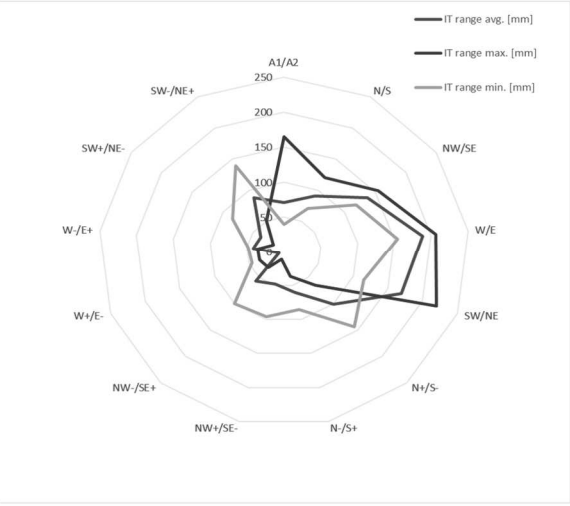

Fig. 12 *Measured values for SLM technology, sample shape full P, and their graphical comparison in polar view*

AREA	IT range min. [mm]	IT range avg. [mm]	IT range max. [mm]	ITx min	ITx average	ITx max
A1/A2	69	171	272	IT10	IT12	IT13
N/S	15	62	109	IT7	IT10	IT11
NW/SE	36	52	116	IT9	IT10	IT11
W/E	61	4	65	IT10	IT0-4	IT10
SW/NE	0	7	20	IT0-4	IT5	IT7
N+/S-	115	78	50	IT11	IT10	IT9
N-/S+	139	99	31	IT12	IT11	IT8
NW+/SE-	48	36	27	IT9	IT9	IT8
NW-/SE+	140	79	0	IT12	IT10	IT0-4
W+/E-	109	69	23	IT11	IT10	IT8
W-/E+	193	139	76	IT12	IT12	IT10
SW+/NE-	113	97	58	IT11	IT11	IT10
SW-/NE+	156	144	130	IT12	IT12	IT11
Average	92	80	75	IT11	IT10	IT10
min	0	4	0	IT0-4	IT0-4	IT0-4
max	193	144	130	IT12	IT12	IT11

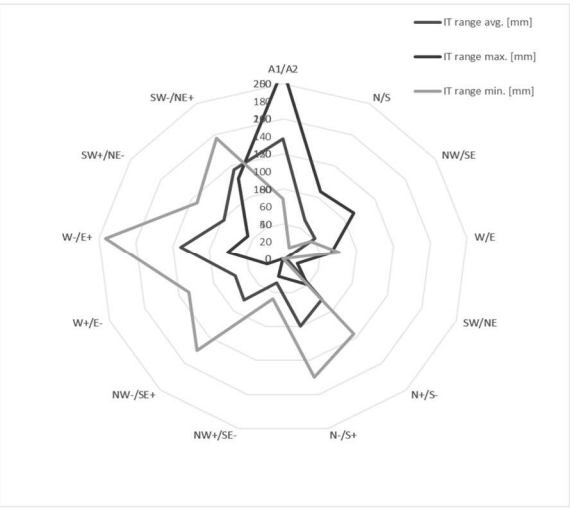

Fig. 13 *Measured values for SLM technology, the shape of hole D sample, and their graphical comparison in polar view*

AREA	IT range min. [mm]	IT range avg. [mm]	IT range max. [mm]	ITx min	ITx average	ITx max
A1/A2	63	137	202	IT10	IT12	IT12
N/S	39	76	136	IT9	IT10	IT12
NW/SE	46	73	114	IT9	IT10	IT11
W/E	39	90	113	IT9	IT11	IT11
SW/NE	48	88	120	IT9	IT11	IT11
N+/S-	129	76	22	IT11	IT10	IT8
N-/S+	139	91	41	IT12	IT11	IT9
NW+/SE-	101	45	32	IT11	IT9	IT8
NW-/SE+	146	119	32	IT12	IT11	IT8
W+/E-	126	67	21	IT11	IT10	IT8
W-/E+	164	101	36	IT12	IT11	IT9
SW+/NE-	140	76	48	IT12	IT10	IT9
SW-/NE+	161	84	15	IT12	IT11	IT7
Average	103	86	72	IT11	IT11	IT10
min	39	45	15	IT9	IT9	IT7
max	164	119	136	IT12	IT11	IT12

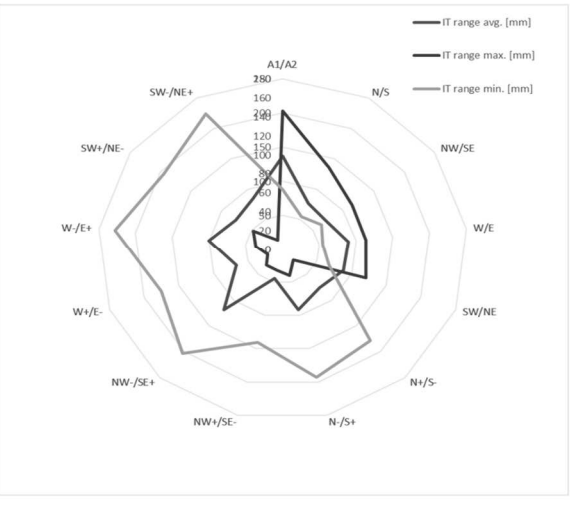

Fig. 14 *Measured values for SLM technology: the shape of the sample with Z threads and their graphical comparison in polar view*

AREA	IT range min. [mm]	IT range avg. [mm]	IT range max. [mm]	ITx min	ITx average	ITx max
A1/A2	96	180	230	IT11	IT12	IT13
N/S	21	1	13	IT8	IT0-4	IT7
NW/SE	6	4	12	IT5	IT0-4	IT6
W/E	83	72	62	IT11	IT10	IT10
SW/NE	101	87	66	IT11	IT11	IT10
N+/S-	126	117	106	IT11	IT11	IT11
N-/S+	97	76	38	IT11	IT10	IT9
NW+/SE-	102	85	65	IT11	IT11	IT10
NW-/SE+	97	79	61	IT11	IT10	IT10
W+/E-	119	90	28	IT11	IT11	IT8
W-/E+	136	114	81	IT12	IT11	IT10
SW+/NE-	111	95	67	IT11	IT11	IT10
SW-/NE+	152	133	89	IT12	IT12	IT11
Average	96	87	71	IT11	IT11	IT10
min	6	1	12	IT5	IT0-4	IT6
max	152	133	106	IT12	IT12	IT11

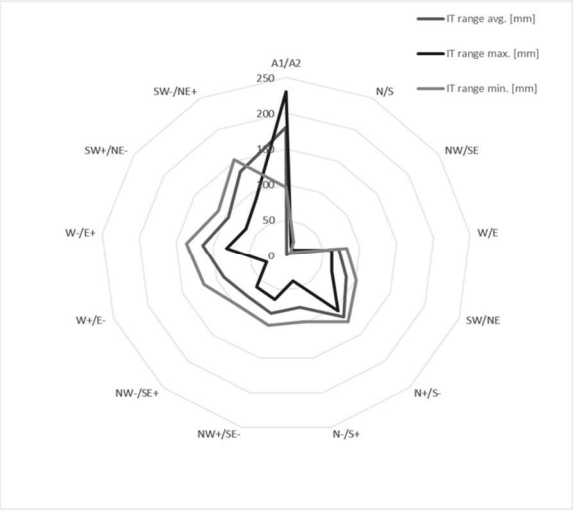

Fig. 15 *Measured values for ADAM technology, sample shape solid P, and their graphical comparison in polar view*

AREA	IT range min. [mm]	IT range avg. [mm]	IT range max. [mm]	ITx min	ITx average	ITx max
A1/A2	69	171	272	IT10	IT12	IT13
N/S	15	62	109	IT7	IT10	IT11
NW/SE	36	52	116	IT9	IT10	IT11
W/E	61	4	65	IT10	IT0-4	IT10
SW/NE	0	7	20	IT0-4	IT5	IT7
N+/S-	115	78	50	IT11	IT10	IT9
N-/S+	139	99	31	IT12	IT11	IT8
NW+/SE-	48	36	27	IT9	IT9	IT8
NW-/SE+	140	79	0	IT12	IT10	IT0-4
W+/E-	109	69	23	IT11	IT10	IT8
W-/E+	193	139	76	IT12	IT12	IT10
SW+/NE-	113	97	58	IT11	IT11	IT10
SW-/NE+	156	144	130	IT12	IT12	IT11
Average	92	80	75	IT11	IT10	IT10
min	0	4	0	IT0-4	IT0-4	IT0-4
max	193	144	130	IT12	IT12	IT11

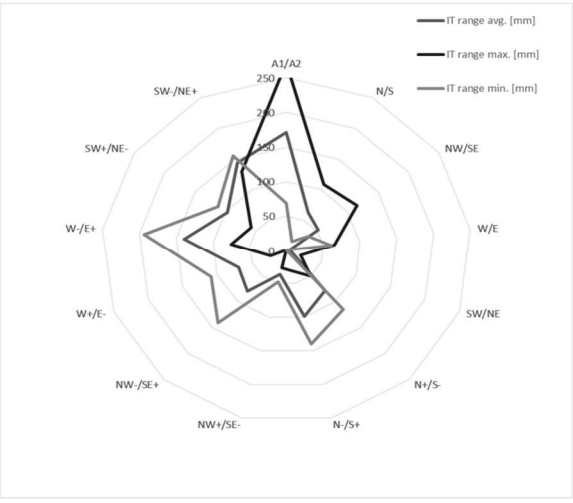

Fig. 16 *Measured values for ADAM technology: shape of hole D sample and their graphical comparison in polar view*

AREA	IT range min. [mm]	IT range avg. [mm]	IT range max. [mm]	ITx min	ITx average	ITx max
A1/A2	106	55	31	IT11	IT10	IT8
N/S	15	1	34	IT7	IT0-4	IT9
NW/SE	8	21	41	IT5	IT8	IT9
W/E	67	32	5	IT10	IT8	IT0-4
SW/NE	84	62	35	IT11	IT10	IT9
N+/S-	88	47	11	IT11	IT9	IT6
N-/S+	196	57	55	IT12	IT10	IT10
NW+/SE-	132	43	43	IT12	IT9	IT9
NW-/SE+	140	100	71	IT12	IT11	IT10
W+/E-	161	77	17	IT12	IT10	IT7
W-/E+	152	109	31	IT12	IT11	IT8
SW+/NE-	202	60	27	IT12	IT10	IT8
SW-/NE+	220	73	45	IT13	IT10	IT9
Average	121	57	34	IT11	IT10	IT9
min	8	1	5	IT5	IT0-4	IT0-4
max	220	109	71	IT13	IT11	IT10

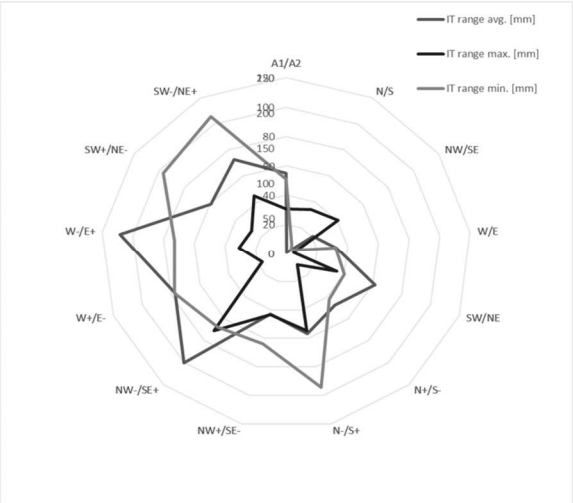

Fig. 17 *Measured values for ADAM technology Z-threaded sample shape and their graphical comparison in polar view*

Samples produced using two different technologies were compared and the IT degree of accuracy of each sample was determined. The sample produced by SLM technology had an average degree of IT accuracy in the range of IT11 to IT12. It achieved the best values for a sample with holes and

threads. The full sample showed a degree worse accuracy quality. The best results were achieved by the full sample. Hole and threaded samples achieved similar IT accuracy values. ADAM technology achieved better results than the studied technologies, with values ranging from IT11 to IT12, with the best results achieved by the threaded sample. Samples with holes and full had similar IT accuracy values. Surfaces that are parallel to the Z-axis show far higher accuracy in samples than inclined surfaces, where IT accuracy of 0-4 is achieved with ADAM technology.

5 Conclusions

The paper presents the results of analyses focused on the working accuracy and surface roughness of 3D objects made of 17-4PH material produced through the Atomic Diffusion Additive Manufacturing ADAM process patented by Markforged Inc. with subsequent comparison with the Selective Laser Melting SLM process. The analysis aims to expand knowledge of the ADAM process, which analyzes the basic characteristics of working accuracy to implement the ADAM process in the industry. The given ADAM process is currently minimally analyzed, despite the amount of added values and positive features of the process.

The results that were found through the conducted experiments will help determine the efficiency, accuracy, quality, and reliability of individual technologies. The experiment was divided into three parts, in which surface texture, surface roughness, and working accuracy were examined. The surface texture experiment analyzes the surface of samples created using two technologies, with individual surfaces created in different directions. The experiment helped determine the technology that scored best in terms of surface texture scanning, whereas ADAM technology was better. SLM technology had significantly worse properties and for A- surfaces it contained supports that required additional post-process activities for removal. During the surface analysis, the parameters of directness (Pa), roughness (Ra), and wavyness (Wa) were determined. ADAM technology achieved better results, on the contrary, SLM technology had unsatisfactory values of the quality of the final surface. With dimensional accuracy, all samples were subjected to complex measurements of individual areas, while the resulting IT accuracy in which individual samples are made was determined from the measured results. The sample produced using ADAM technology performed better, followed by SLM technology. The lowest IT accuracy was recorded by ADAM technology, while its resulting values differed from the SLM process by up to 3 degrees.

The resulting evaluation of experiments comparing two additive manufacturing technologies focused on metallic materials showed that the application of ADAM technology is more suitable for the production of components of complex geometric shapes. This technology has stood up to all experiments as the best, producing components with excellent IT accuracy, and surface texture and minimizing post-processing activities. The research has benefits in the field of metal additive manufacturing in terms of comparing the two most advanced and widely used technologies in terms of accuracy, hardness, and surface design. The history of successful cases of the ADAM process is gradually growing, and its positive qualities are gradually implemented in the production process. These types of products have a lower weight due to the internal grid, so the material does not have a full density and is therefore an excellent alternative for environmental applications. The filament-based ADAM process was conceived as a viable economical alternative for the production of elements with simpler material management than additive manufacturing based on metal powders.

Further research activities could be aimed at investigating the influence of different heat treatments on microstructure, and static and dynamic performance properties.

Acknowledgement

This research was funded by the University of Žilina project VEGA 1/0520/21 Research of the integrity of surfaces created by the additive process of atomic diffusion of metal-elastomer fibers with post-process of productive machining, next project KEGA 063ŽU-4/2021: "Integration of detection-visualization technologies for innovative additive manufacturing technologies as an online tool for creative and critical thinking".

References

[1] GALATI, M.; MINETOLA, P.; Analysis of Density, Roughness, and Accuracy of the Atomic Diffusion Additive Manufacturing (ADAM) Process for Metal Parts. *Materials* 2019, 12, 4122; doi:10.3390/ma12244122, 1-15

[2] LEE, H.; LIM, C.H.J.; LOW, M.J.; THAM, N.; MURUKESHAN, V.M.; KIM, J.-J. Lasers in additive manufacturing: an overview. I*nt. J. Precis. Angl. Manuf. Green technol.* 2017, 4, 307–322.

[3] BIAMINO, S.; PENNA, A.; ACKELID, U.; SABBADINI, S.; TASSA, O.; FINO, P.; PAVESE, M.; GENNARO, P.; BADINI, C. Electron beam melting of the alloy Ti–48Al–2Cr–2Nb: Investigation of microstructure and

mechanical properties. *Intermetallic Substances* 2011, 19, 776–781.

[4] GIBSON, I.; ROSEN, D.W.; STUCKER, B. AM technologies; Springer: New York, NY, USA, 2015.

[5] SAADLAOUI, Y.; MILAN, J.-L.; ROSSI, J.-M.; CHABRAND, P. Topology optimization and additive manufacturing: Comparison of design methods using industry codes. *J. Manuf. Syst.* 2017, 43, 178–186.

[6] KRUTH, J.-P.; LEU, M.-C.; NAKAGAWA, T. Advances in additive manufacturing and rapid prototyping. *CIRP Ann.* 1998, 47, 525–540.

[7] MCALEA, K. Materials and applications for selective laser sintering. In *Proceedings* of the 7th International Conference on Rapid Prototyping, San Francisco, CA, USA, March 31-April 3, 1997; pp. 23-33.

[8] GALATI, M.; IULIANO, L. Literature review on powder-based electron beam melting with a focus on numerical simulations. *Add. Manuf.* 2018, 19, 1–20.

[9] SGAMBATIA, A.; BERGA, M.; ROSSIA, F.; DAURSKIKHB, A.; IMHOFC, B.; DAVENPORTC, R.; WEISS, P.; PEER, M.; GOBERT, T.; MAKAYA, A. URBAN: Lunar base design using 3D printing technologies. In *Proceedings* of the 69th International Astronautical Congress, Bremen, Germany, 1-5 October 2018; pp. 1-9.

[10] CAMPBELL, R.I.; WOHLERS, T. MARKFORGED: *A different approach to metal additive manufacturing*. Available online: http://www.metal-am.com/wp-content/uploads/sites/4/2017/06/MAGAZINE-Metal-AM- Summer-2017-PDF-sp.pdf (accessed 23 July 2019).

[11] MARKFORGED. *Materials*. Available online: https://markforged.com/blog/metal-3d-printing-materials/ (accessed 5 December 2019).

[12] SPENCER, O.O.; YUSUF, O.T.; TOFADE, T.C. The evolution of additive manufacturing technology: a trajectory towards the industrial revolution. *Am. J. Moss. Ind. Eng.* 2018, 3, 80–90.

[13] BHERO, S. Metal injection molding as a possible processing pathway for porous prostheses. *Int. J. Res. Chem. Metall. Civ. Eng.* 2014, 1, 50–53.

[14] WOHLERS, T. Desktop Metal: Vychádzajúca hviezda kovovej aditívnej výroby sa zameriava na rýchlosť, náklady a veľkoobjemovú výrobu. *Kovová AM*. Online: http://www.metal-am.com/wp-content/uploads/sites/4/2017/06/MAGAZINE- Kov-AM-Leto-2017-PDF-sp.pdf (prístup k 23. júlu 2019).

[15] GONZALEZ-GUTIERREZ, J.; CANO, S.; SCHUSCHNIGG, S.; COCOON, C.; SAPKOTA, J.; HOLZER, C. Additive manufacturing of metal and ceramic components by extrusion of highly filled polymer materials: an overview and future perspectives. *Materials* 2018, 11, 840.

[16] MARKFORGED. *Stainless steel 17-4 PH*. Material datasheet. Available online: https://static.markforged.com/download/markforged_datasheet_17-4_ph_stainless_steel.pdf (accessed 5 December 2019).

[17] TIMKO, P.; HOLUBJAK, J.; BECHNÝ, V.; NOVÁK, M.; CZÁN, A.; CZÁNOVÁ, T.; Surface Analysis and Digitization of Components Manufactured by SLM and ADAM Additive Technologies, *Manufacturing Technology* 2023, 23(1):127-134, DOI: 10.21062/mft.2023.008.

[18] SPIERINGS, A.B.; SCHNEIDER, M.; EGGENBERGER, R. Comparison of density measurement techniques for additively manufactured metal parts. *Rapid prototype*. J. 2011, 17, 380–386.

[19] TIMKO, P.; CZÁNOVÁ, T.; CZÁN, A.; SLABEJOVÁ, S.; HOLUBJAK, J.; CEDZO, M.; Analysis of Parameters of Sintered Metal Components Created by ADAM and SLM Technologies, *Manufacturing Technology* 2022, 22(3):347-355, DOI: 10.21062/mft.2022.032

[20] HALL, C.; HAMILTON, A. Porosity of building limestones: Using solid density to assess data quality. *Mother. Struct.* 2016, 49, 3969–3979.

[21] PANNETON, R.; GROŠ, E. Missing mass method for measuring the open porosity of porous solids. *Acta Acust.* United Acust. 2005, 91, 342–348.

[22] KOZOVÝ, P.; ŠAJGALÍK, M.; DRBÚL, M.; HOLUBJÁK, J.; MARKOVIČ, J.; JOCH, R.; BALŠIANKA, R.; Identification of Residual Stresses after Machining a Gearwheel Made by Sintering Metal Powder, Manufacturing Technology 2023, 23(4):468-474, DOI: 10.21062/mft.2023.054

[23] MESICEK, J.; RICHTAR, M.; PETRU, J.; PAGAC, M.; KUTIOVA, K.; Complex View to Racing Car Upright Design and Manufacturing, *Manufacturing Technology* 2018, 18(3):449-456 DOI: 10.21062/ujep/120.2018/a/1213-2489/MT/18/3/449

[24] MINETOLA, P.; GALATI, M.; IULIANO, L.; ATZENI, E.; SALMI, A. Using self-replicated parts to improve the design and accuracy of an inexpensive 3D printer. *CIRP Procedure* 2018, 67, 203–208.

[25] MINETOLA, P.; GALATI, M. The challenge of increasing the dimensional accuracy of a cheap 3D printer using self-replicable parts. *Add. Manuf.* 2018, 22, 256–264.

[26] ISO. *ISO 286-1:1988*—ISO system of limits and fits. Part 1: Basis of tolerances, deviations and appropriateness; International Organization for Standardization (ISO): Gevena, Switzerland, 1988.

[27] ISO. *ISO 10360-2:2009* – Geometric specifications of a product (GPS) – Acceptance and verification tests for coordinate measuring instruments (CMM). Part 2: CMM used to measure linear dimensions; International Organization for Standardization (ISO): Gevena, Switzerland, 2009.

[28] CONDRUZ, M.R.; PARASCHIV, A.; PUSCASU, C. Effect of heat treatment on hardness and microstructure of ADAM produced 17-4 PH. *Turbo* 2018, V, 39–45.

[29] VIOLANTE, M.G.; IULIANO, L.; MINETOLA, P. Design and manufacture of fixtures for loose components using selective laser sintering. *Rapid prototype. J.* 2007, 13, 30–37.